The Reward-Attention Circuit Model: Nicotine's Influence on Attentional Focus and Consequences on Attention Deficit Hyperactivity Disorder

Karine Guimarães[a], Daniele Q.M. Madureira[a], Alexandre L. Madureira[a,b,*]

[a]*Laboratório Nacional de Computação Científica, Av. Getúlio Vargas 333, Petrópolis–RJ, Brazil*
[b]*Fundação Getúlio Vargas, Praia de Botafogo 190, Rio de Janeiro - RJ, Brazil*

Abstract

In this work we investigate the influence that nicotine exerts on attention focusing, modeling the coupling of reward and thalamocortical circuits. Each neuron in the neural networks that replicate such circuits is described by a carefully designed coupled system of nonlinear differential equations that details essential neurophysiological properties.

Computer simulations of the reward-attention circuit reflects the spiking behavior of each individual neuron in the network, under the presence or absence of nicotine. It becomes clear that changes in the dopaminergic levels in the reward circuit due to nicotine strongly influences the nigral dopaminergic activity, that modulates the thalamocortical filtering mechanism.

Our results indicate that nicotine strengthens the attentional focus on a particular stimulus, decreasing the smoker's mental flexibility. Also, the simulations highlight aspects of clinical inattention symptoms, particularly in the attention deficit hyperactivity disorder. They show why patients suffering from attentional lability might improve the attentional focus when exposed to nicotine.

Keywords: Nicotine, Dopamine, Attention, ADHD, Computational neuroscience

*Corresponding author

Email addresses: kdamasio@lncc.br (Karine Guimarães), daniele@lncc.br (Daniele Q.M. Madureira), alm@lncc.br (Alexandre L. Madureira), alexandre.madureira@fgv.br (Alexandre L. Madureira)

1. Introduction

While substance dependence is the outcome of highly complex interactions, changes in the amount of dopamine in the reward circuit has proved to be an important addictive culprit of substance abuse. Associated with the pleasures triggered by natural rewards, this neural circuit is the natural basis for the phenomena related to the addiction. In fact, dopamine is a neurotransmitter that plays a crucial role in the motivational control. The main sources of dopamine in the cerebral cortex and subcortical regions are the ventral midbrain dopaminergic neurons located in the pars compacta region of the *substantia nigra* (SN) (see Table 1 for a complete listing of acronyms) and in the *ventral tegmental area* (VTA) [1, 2].

Tobacco addiction is a multistage process involving persistent cycles of chronic smoking. It is associated with long-lasting effects of nicotine — the main addictive substance in the tobacco — on the reward circuit [3]. However, despite its perverse effects, the use of nicotine can be therapeutic [4]. Clinical trials have shown that nicotine may improve the cognitive performance in a variety of groups, including non-smoking healthy adults. The improvement is perceived throughout a series of cognitive tasks, in particular, attention focusing [4, 5]. Moreover, several evidences suggest that the use of nicotine diminishes inattention symptoms in patients with *attention deficit hyperactivity disorder* (ADHD) [6]. Because of its potential therapeutic value in states characterized by attentional dysfunction [7], neuronal mechanisms underlying the attentional functions affected by nicotine are of increasing interest. However, the neural mechanisms through which nicotine acts to modulate the attention focusing are not yet fully elucidated.

Here, we propose a neurocomputational model to investigate the nicotine's influence on attention, through its action on the reward and thalamocortical circuits. Our approach highlights the importance of subcortical systems in attentional mechanisms — in particular, the dopaminergic role in the thalamocortical circuit. The association between nicotine and dopaminergic rewarding mechanisms has already been addressed before through computational models [8, 9, 10, 11]. Our work, however, follows a particular direction since it considers the coupling of the rewarding and thalamocortical circuits as an essential site for exploring how nicotine affects the attentional focus.

Thalamocortical circuits are known to select environmental stimuli. By a negative feedback mechanism involving cortical, thalamic and reticular thalamic neurons, they play an essential role in the focusing of attention [12, 13].

Indeed, pathological variations in this circuit's dopaminergic level can promote attentional deficits in patients with Parkinson's disease and ADHD, due to the modulation of thalamic areas, by neural projections from the SN [14]. Accordingly, decreases in the level of mesothalamic dopamine exaggerates the focusing, diminishing thus the cognitive flexibility.

Justified by synaptic projections the *nucleus accumbens* (NAcc) sends to the SN [15], our neurocomputational model investigates the influence of nicotine on attention through the interaction between the reward and thalamocortical circuits. More specifically, computational simulations of the reward-attention circuit model provide numerical results that describe the neurons' spikes in the neural network. Each neuron is modeled by a system of differential equations that incorporates these cells' electrophysiological characteristics both in the presence or absence of nicotine.

Now, we outline the contents of this article. Sections 2 and 3 describe the neurophysiology of the reward-attention circuit model, and then its modeling. Section 4 explains the design of the computational simulations. The results of the simulations are presented in Section 5, followed by a discussion in Section 6. Finally, the Appendix contains tables describing the acronyms and a glossary of the parameters

2. The Reward Attention Circuit model

Based on neurophysiological and neurochemical aspects, the reward-attention circuit model addresses the interaction between the reward and thalamocortical circuits, to explore the focusing of attention under the influence of nicotine. The corresponding architecture is shown in Figure 1.

Here, the reward circuit is represented by the *prefrontal cortex* (PFC), and the VTA and NAcc regions. The thalamocortical circuit includes the PFC, thalamus and the *thalamic reticular nucleus* (TRN). The communication between these circuits is established through the SN that inhibits the TRN and receives inhibitory projections from the NAcc. The *pedunculopontine nucleus* (PPN) , in turn, excites the SN.

Intrinsic membrane properties regulate the activity of dopaminergic neurons in the VTA. The tonic firing is driven by a *pacemaker current*, which induces the neuron to fire spontaneously and independently of external stimuli, and such spontaneous spiking mode provides the postsynaptic neurons in the NAcc with a stable level of dopamine.

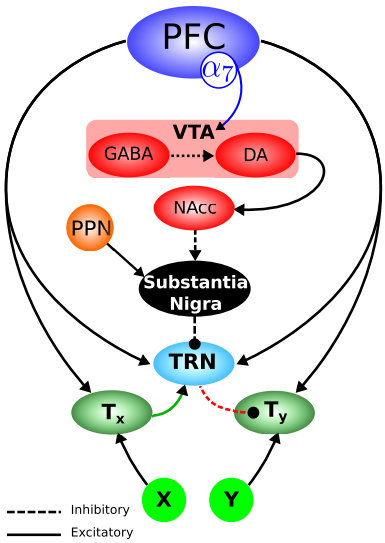

Figure 1: Reward Attention Circuit architecture: excitatory synapses (continuous lines), inhibitory synapses (dotted lines).

Both electrical activity increase and dopamine release of the VTA dopaminergic neurons are heavily regulated by the activation of NMDA receptors, and such mechanisms are crucial for the induction of *long term potentiation* (LTP) of these neurons. In particular, NMDA receptors are involved in mediating phasic spikes [16, 17], that are associated with a greater release of dopamine into the NAcc, compared with the outflow due to the tonic spiking mode [18, 19, 20].

In our model, nicotine is responsible for activating the reward circuit. The psychopharmacological mechanism involved is the direct action of nicotine on the *nicotinic acetylcholine receptors* (nAChR). There are two types of nicotinic receptors in the reward circuitry, the α_7 and the $\alpha_4\beta_2$, which, for simplicity, we denote by α_7^+ and α_7^-. The nicotine acts on the axonic terminals of PFC neurons and, as a result, glutamate is released into the VTA.

In the VTA, nicotinic and glutamatergic receptors are activated by nicotine and glutamate, respectively, stimulating thus the GABAergic interneurons and the dopaminergic neurons. The GABAergic interneurons activity lasts only a few minutes, due to the α_7^- receptors. The α_7^- becomes inactive faster than the α_7^+ ones. Dopaminergic neurons, in turn, continue to receive excitatory inputs from cortical glutamatergic neurons, even when the

inhibitory GABAergic interneuron stimuli ceases to exist.

The glutamatergic action on NMDA receptors lasts considerably longer than on the AMPA receptors. However, under normal physiological conditions, the NMDA receptor is partially blocked by magnesium ions (Mg^{++}). As both the presynaptic and the postsynaptic cells must be active for the NMDA current to flow, the presence of these receptors is supposed to be necessary for many types of long-term changes in synapses that presumably encode memories. The glutamatergic action enhanced by nicotine activates NMDA receptors in the VTA dopaminergic neurons [21]. One of the ions carried by the NMDA current is calcium, which is a major player in long-term neural changes. This current is also thought to play a role in maintaining persistent activity required for short-term memory [22].

The influx and subsequent increase in the concentration of intracellular Ca^{++} amplifies the hyperpolarization phase of the action potential, which is essential for the occurrence of the burst spike mode [23, 24]. Thus, the interaction between the membrane's ionic currents and the afferent synaptic inputs contributes to accelerate or decelerate the dopaminergic neuron firing activity, depending on the need to optimize the dopamine release. VTA dopaminergic neurons project on the NAcc GABAergic neurons — the final site currently associated with the pleasure sensation triggered by nicotine.

From there, the NAcc and SN connects the reward and the thalamocortical circuits, and also inhibit the dopaminergic neurons in the SN. Since the NAcc projections are inhibitory, the SN and NAcc behaviors are inversely proportional, i.e. the SN becomes more (less) active as the NAcc becomes more (less) inhibited.

On the other hand, assume that two external stimuli x and y reach the neighboring thalamic regions T_x and T_y through glutamatergic excitatory pathways. Once stimulated, T_x activates the NRT through an ascending glutamatergic projection, with the PFC as the final destination. Since we do not explicitly model the cortical region related to the thalamocortical circuit, such excitatory projection ends up in the TRN. Also, through an excitatory glutamatergic descending pathway, the cortical region increases the activation of T_x and also sends collateral axons to the TRN.

Once activated, the TRN, through its GABAergic projection, inhibits the thalamic region T_y in the neighborhood of T_x. Our model addresses the TRN area stimulated by the thalamic region T_x and the PFC. Therefore, the thalamocortical circuit activation by an external stimulus x excites a central thalamic region T_x and inhibits its neighborhood, represented by the region

T_y. Such a mechanism permeates the formation of an attentional focus (for further details see [14]).

Furthermore, the TRN receives dopaminergic inhibitory projections from the SN. Accordingly, a rise in the nigral dopamine release contributes for the TRN deactivation, thus leading to a more active thalamic region T_y, and to a more flexible attentional focus. Conversely, a reduction in the SN dopaminergic level makes the TRN more excited, and increases the inhibition on T_y.

Overall, our working hypothesis is that the NAcc activity influences the SN behavior, which modulates the focusing of attention, and that the presence of nicotine is powerful enough to bias the NAcc activation.

3. Mathematical formulation

From a mathematical point of view, we model the neurons using *Integrate and Fire* equations [25]. Such modeling is suitable for network simulations, and can be adapted to simulate a broad class of neuronal behavior. We consider one-compartment neurons with electric potential V. [14, 26, 27, 28] As usual, the membrane of the neuron is modeled by electric capacitors in parallel with a series of resistors, which represent ions channels and synaptic connections. In general, the membrane equation is described by

$$\begin{cases} C_i \dfrac{\mathrm{d}V_i}{\mathrm{d}t} = \displaystyle\sum_{j=1}^{J_i} \mathrm{I}_i^j + I_{\text{ext}}, \quad t \in (0, T] \\ V_i(0) = V_i^0 \end{cases} \tag{1}$$

where $i = 1, \ldots, n$ refers to each of the n neurons in the network, C_i denotes their capacitances, and J_i is the number of ionic currents being modeled in the ith neuron, while I_{ext} model external currents. The currents are defined as $\mathrm{I}_i^j = g_j(V_i)(E_j - V_i)$, where g_j is the conductance and E_j is the Nernst potential corresponding to the jth ion. The physiological characteristics of each neuron is modeled by the conductance g_j, which might not only depend on t explicitly, but also on previous values of V_i itself, through, for instance, differential equations.

We assume that spikes are due to voltage-dependent currents — the sodium current, which depolarizes the neuron, and the potassium current I_{K}, which restores the cellular membrane potential — and synaptic currents

that contribute to the excitation or inhibition of the cell, according to the behavior of the presynaptic neurons. Also, we consider the leak current, which lumps other currents not explicitly modeled.

As an exception, the sodium current is not represented as described above. It is activated by the action of the Heaviside function $\Theta : \mathbb{R} \to \{0, 1\}$, defined by

$$\Theta(x) = \begin{cases} 1 & \text{if } x \geqslant 0 \\ 0 & \text{if } x < 0, \end{cases}$$

applied to $(V_i - \theta_{\mathrm{Na}})$, where θ_{Na} is a fixed constant.

After a spike, the conductance g_{k} of the restoring current I_{K} increases rapidly, bringing the neuron back to a resting potential. This process is described in general by

$$\frac{\mathrm{d}g_{\mathrm{k}}}{\mathrm{d}t} = \frac{\beta_{\mathrm{K}}\Theta(V - \theta_{\mathrm{Na}}) - g_{\mathrm{K}}}{\tau_{\mathrm{K}}} \quad \text{for } t \in (0, T], \qquad g_{\mathrm{K}}(0) = g_{\mathrm{K}}^0$$

where the constants g_{k}^0, β_{K} and τ_{k} are the initial state of g_{k}, the variation rate of g_{k}, and the time constant associated with the potassium channel. The above equation actually holds for all neurons, with V being replaced V_i, g_{k} replaced by $g_{\mathrm{k,i}}$, etc.

The synaptic conductances g_{sin} reflect the level of a neurotransmitter released by the presynaptic neuron. It is described by

$$g_{\mathrm{sin}}(t) = \hat{g}_{\mathrm{sin}} \sum_j (t - t_j) \exp\left(-\frac{t - t_j}{t_p}\right) \Theta(t - t_j),$$

where the times t_j, with $j = 1, \ldots, \mathcal{N}$, are the spiking times of a presynaptic cell, while the constant $\hat{g}_{\mathrm{sin}}$ is the maximal conductance. We denote by t_p the peak time for the alpha function, and it assumes the values t_{pe} and t_{pi} for excitatory and inhibitory synapses, respectively.

All the neurons in the network, therefore, present sodium and potassium ionic currents, and synaptic currents. However, each neuron receives distinct neurotransmitters according to their specific afferents. Besides the currents involved in the action potential, there are those associated with particular properties of each neuron. Next, we describe them.

The nicotine acts on the cortical neuron through the α_7 receptors. The variation in the number of activated α_7^+ receptors is given by the solution of

the equation

$$\frac{\mathrm{d}\alpha_7^+}{\mathrm{d}t} = k_1\alpha_7^- n_{\mathrm{ic}} - k_2\alpha_7^+ \quad \text{for } t \in (0,T], \qquad \alpha_7^+(0) = \alpha_7^{+,0},$$

where $\alpha_7^{+,0}$, α_7^-, k_1 and k_2 are constants, and $n_{ic} : (0,T] \to \mathbb{R}$ is solution for the following differential equation

$$\frac{\mathrm{d}n_{ic}}{dt} = -Mn_{\mathrm{ic}} \quad \text{for } t \in (0,T], \qquad n_{\mathrm{ic}}(0) = n_{\mathrm{ic}}^0, \tag{2}$$

where M e $n_{\mathrm{ic}}^0 \in \mathbb{R}$.

The NMDA current in the VTA dopaminergic neurons is triggered by the conductance $g_{\mathrm{NMDA}} = \bar{g}_{\mathrm{NMDA}}\, h(t) B(V_3)$, where V_3 is the voltage of the VTA dopaminergic neuron, and $h(t)$ denotes the fraction of open channels and satisfies

$$\frac{\mathrm{d}h}{\mathrm{d}t} = a_{\mathrm{r}}(1-h)\,\mathcal{T}(V_1) - a_{\mathrm{d}}h \quad \text{for } t \in (0,T], \qquad h(0) = h^0.$$

The parameters $a_{\mathrm{r}} = 0,072\ \mathrm{mM}^{-1}\mathrm{ms}^{-1}$ and $a_{\mathrm{d}} = 0,0066\ \mathrm{ms}^{-1}$ characterize the rate of increase and decay of the conductance, respectively. The function $\mathcal{T}$ depends on the cortical neuron as follows

$$\mathcal{T}(V_1) = \frac{\mathcal{T}_{\max}}{1 + e^{-(V_1 - V_{\mathcal{T}})/k_{\mathrm{p}}}},$$

where $\mathcal{T}_{\max} \in \mathbb{R}$ is the maximum concentration of neurotransmitters in the synaptic cleft, V_1 is the voltage of the cortical neuron, $k_{\mathrm{p}} = -5\mathrm{mV}$ is the decay of neurotransmitters and $V_{\mathcal{T}} = -10\mathrm{mV}$ represents the value at which the function is activated.

The term $B(V_3)$ models the blocking of the ion channel by magnesium [29],

$$B(V_3) = \frac{1}{1 + e^{-(V_3 - V_{\mathrm{T}})/16.13}},$$

where $V_{\mathrm{T}} = 16.13 \ln\left(\frac{[Mg^{++}]}{3.57}\right)$ is the half activation.

As the NMDA receptors open, calcium ions enter the cell. The calcium conductance $g_{\mathrm{c}} = \bar{g}_{\mathrm{c}}[Ca]$ is proportional to the intracellular calcium, with the constant rate $\bar{g}_{\mathrm{c}}$. The equation describing the concentration of calcium in the cell is given by

$$\frac{\mathrm{d}[Ca]}{\mathrm{d}t} = \frac{\beta_{[\mathrm{Ca}]}\,\Theta(V_3 - \theta_{\mathrm{Na}}) - [Ca]}{\tau_{[\mathrm{Ca}]}} \quad \text{for } t \in (0,T], \qquad [Ca](0) = [Ca]^0, \tag{3}$$

where $[Ca]^0$ is the initial condition, and the constants $\beta_{[\mathrm{Ca}]}$ and $\tau_{[\mathrm{Ca}]}$ represent the rate of the calcium concentration variation and a time constant. The function $\Theta(V_3 - \theta_{[\mathrm{Na}]})$ raises the calcium concentration whenever there is a neural spike.

When the intracellular calcium concentration reaches a threshold value $\theta_{[\mathrm{Ca}]}$, the K^+ ionic channels of the hyperpolarizing current I_{ahp} opens up, and the conductance g_{ahp} increases at the rate β_{ahp}. This is represented by the equation,

$$\frac{\mathrm{d}g_{\mathrm{ahp}}}{\mathrm{d}t} = \frac{\beta_{\mathrm{ahp}}\,\Theta([Ca] - \theta_{[\mathrm{Ca}]}) - g_{\mathrm{ahp}}}{\tau_{\mathrm{ahp}}} \quad \text{for } t \in (0, T], \qquad g_{\mathrm{ahp}}(0) = g^0_{\mathrm{ahp}},$$

where τ_{ahp} it is a time constant.

The pacemaker current is described by $I_{\mathrm{pm}} = g_{\mathrm{pm}}(V_3 - E_{\mathrm{pm}})$, where g_{pm} and E_{pm} are constants.

Dopamine inhibits the TRN neuron, and we assume that the final target of the dopaminergic action is the calcium-dependent potassium channel [30]. Its conductance $g_{\text{k-c}} = \hat{g}_{\mathrm{c}}\, D_4^*\, S([Ca])$ suffers the dopaminergic influence through the receptor D_4^* and depends on the intracellular calcium concentration. In the above formula, $\hat{g}_{\mathrm{c}}$ is a proportionality constant and the sigmoid function $S([Ca])$ describes the increase in intracellular calcium concentration by virtue of the neural spike,

$$S([Ca]) = \frac{1}{1 + \exp(-\alpha[Ca])},$$

where the constant α controls the slope of S.

The calcium concentration is described as in (3), with V_3 being replaced by V_{10}. Note that $g_{\text{k-c}}$ increases and inhibits the cell, if the cell is excited beyond a threshold. The dopaminergic action on the D_4^* receptor represents the ups and downs of the dopaminergic level according to the equation

$$D_4^*(t) = \hat{g}_{\mathrm{d4}} \sum_j (t - t_j) \exp\left(-\frac{t - t_j}{t_{\mathrm{pd}}}\right) \Theta(t - t_j),$$

where t_{pd} stands for the peak time and $\hat{g}_{\mathrm{d4}}$ is the conductance constant of the dopaminergic projection.

The differential equations are discretized in time using the Euler's method. In the Appendix A, Table 2 presents a glossary with all necessary parameter values.

4. Simulation methods

Besides conducting experiments to address the network behavior, we calibrate each neuron separately, according to their specific neurophysiological properties [31], before they are included in the network.

4.1. Baseline case

We start our simulations considering a "healthy" brain, and set the physiological parameters in the "normal" range [13, 14, 23, 24, 31] — such step is important to establish benchmark results. By healthy, we mean an individual with no pathology, whose brain has not been exposed to nicotine and with a normal capacity of attentional focusing. For a normal attentional focus on stimulus x to occur, the thalamic area T_x must be more activated than its neighboring area T_y. However, it is also necessary that the amount of activation in T_y is not much lower than the one occurring in T_x — otherwise, there will appear an hyper attention focusing on x. Besides, the activation of T_y cannot be similar to T_x — otherwise, there will be no attention focusing at all [14].

In this paper we consider that at the baseline case the reward system remains almost inactive, in the absence of nicotine. Therefore, the cortical neuron — in the reward circuit — and the VTA GABAergic neurons present no spikes. On the contrary, the VTA dopaminergic neuron runs a pacemaker activity, delivering to the NAcc a basal level of dopamine. The mesothalamic dopamine from the SN modulates the degree by which the TRN inhibits T_y. Since the projection from the NAcc to the SN is GABAergic, and the SN receives excitatory inputs from the PPN, we indirectly model the PPN behavior, by setting, for the baseline case, a frequency of one spike for every 10 milliseconds. During a 500 milliseconds simulation, the excitatory inputs x, y and the PFC projection in the thalamocortical circuit are represented by periodic in time sequences of 1 spike per millisecond. And, after 100 ms, the TRN neuron receives inhibitory dopaminergic modulation from the SN, and the influence of the nigral dopamine becomes apparent.

4.2. Exposure to nicotine

Next, we designed an experiment addressing the case involving exposition to nicotine. Starting from the baseline case, nicotine is added to the system through the term $n_{\mathrm{ic}}(0)$ in (2). All other parameters are the same as in the baseline case.

Accordingly, both the cortical and the VTA GABAergic neurons become active due to the consumption of nicotine. It is important to remark that, in our model, the influence of nicotine on the VTA GABAergic neuron occurs because of the increased cortical excitatory stimulation triggered by nicotine.

4.3. Implications in ADHD

Our last set of simulations involves the use of nicotine by ADHD patients. To understand the inattention symptoms in ADHD, we consider two antagonistic explanations for their causes: the *high attention focusing* and the *no attention focusing* [14]. The first considers the attentional deficits as resulting from a difficulty, or inability, to shift the attentional focus. Therefore, a mental rigidity makes the attention to focus in only one internal or external stimulus, and the patient is not be able to pay attention in, nor distinguish other stimuli. Conversely, the *no attention focusing* explanation interprets the ADHD inattention symptoms as an excessive displacement of the attentional focus. In this case, attention would be continuously directed to different stimuli, without actually concentrating on anything.

Concerning the SN firing rate in the baseline experiment, it is important to note that low SN spiking rates are associated with the mesothalamic dopaminergic hypoactivity, whereas the opposite case is associated with mesothalamic dopaminergic hyperactivity. Furthermore, the dopaminergic hypoactivity is associated with the mental rigidity observed in both Parkinson's disease and ADHD, while the dopaminergic hyperactivity underlies the defocusing symptoms in ADHD [14].

There are increasing evidences indicating that the PPN is involved in mechanisms enhancing attention [32], reward, and learning [33]. Moreover, the PPN suffers degeneration in human neurodegenerative disorders also characterized by attentional and/or mnemonic deficits, including Parkinson's disease [34, 35]. It has been proposed that PPN has a role in the SN degeneration due to an excitotoxic effect of the glutamatergic synaptic contacts from the PPN into the SN dopaminergic neurons [35, 36].

Thus, variations in the SN spiking frequencies are simulated through changes in the PPN's firing rates. All other parameters are the same as in the baseline case. Departing from the simulation of an ADHD pathological state, nicotine is added to the system.

5. Numerical results

5.1. Baseline case

Our first results refer to the normal attention focusing without nicotine. In Figures 2a–d, we observe the membrane's voltage of the VTA dopaminergic, TRN, T_x and T_y neurons.

The pacemaker current acting on the ATV dopaminergic neuron induces a tonic spiking mode, thus sending a basal level of dopamine to the NAcc, see Figure 2a. During the first 100ms, we prevented the SN neuron from firing, to observe more clearly the influence of dopamine on the TRN after 100ms. Without the influx of dopamine from the SN neurons, the TRN neuron becomes so excited that completely inhibits the neighboring thalamic area T_y. As a consequence, the attentional focus becomes centered on the stimulus x. After 100 ms, however, the activation of the dopaminergic neurons of the SN, and the consequent inhibition on the TRN, enables the activation of T_y, which starts competing with T_x for cortical processing. The balance of such competition is healthy for allowing attentional shifting. Indeed, this is necessary for the cognitive process to occur efficiently.

This experiment provides a baseline reference for our further simulations concerning nicotine and ADHD. Figure 3 presents the spiking frequencies of both T_x and T_y, relative to this baseline case.

5.2. Exposure to nicotine

In the sequel, our results concerns an individual whose brain is exposed to nicotine. So, starting from the baseline case, nicotine is added to the system. Consequently, the VTA dopaminergic neuron starts to receive cortical glutamatergic and VTA GABAergic stimuli. In comparison with the baseline case, shown in Figure 2a, they become more excited, thus increasing the level of dopamine that is released into the NAcc, as we can observe in Figure 4a. It is important to note that such mechanism results in a reward sensation.

With the cessation of the GABAergic inhibition, and the altogether continuity of cortical excitatory glutamatergic stimulation on the VTA dopaminergic neuron, there plausibly occurs a long term potentiation [9]. As a consequence, there occurs a change in the spiking mode of such VTA neurons, who start to fire in bursts. It happens due to the activation of the NMDA receptors, the calcium current and the hyperpolarizing current. Figures 4b–d depict the behavior of the SN, T_x and T_y neurons.

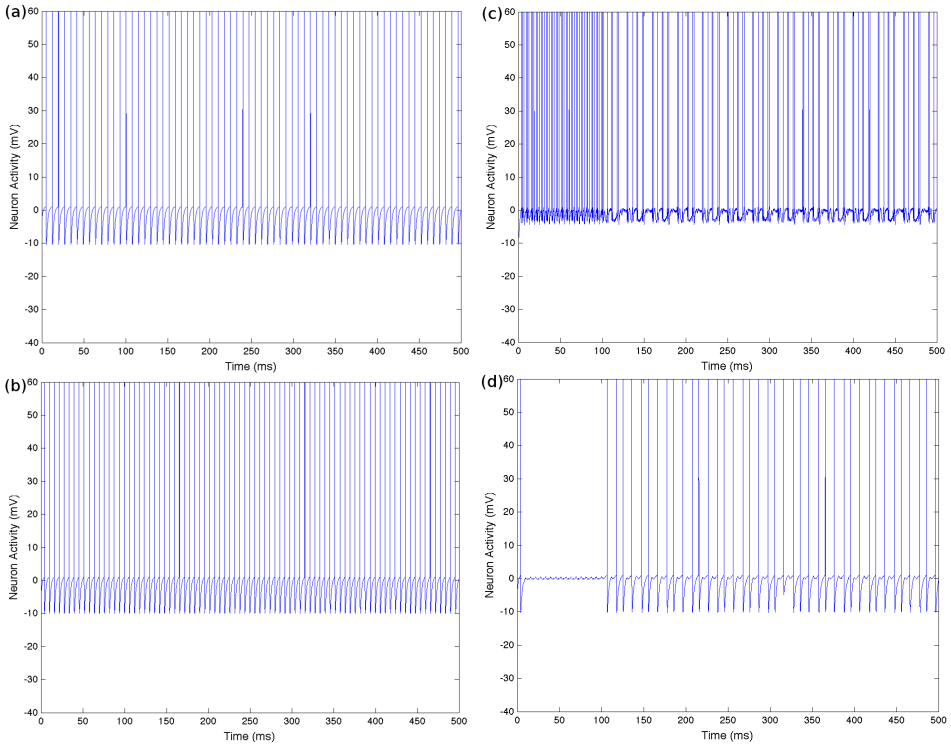

Figure 2: Attention focusing in a healthy individual, without nicotine: (a) VTA dopaminergic neuron under a pacemaker activity; (b) TRN presents inhibition due to dopaminergic action after 100 ms; (c) Behavior of T_x; (d) Behavior of T_y.

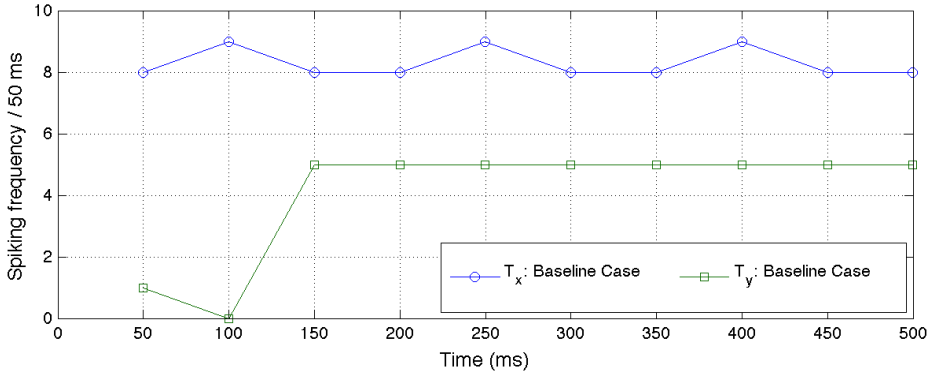

Figure 3: Baseline case. Spiking frequencies of T_x and T_y.

Note that there is no noticeable change in the behavior of T_x relative

to the baseline situation shown in Figure 2c. The comparison between T_x and T_y — shown in Figure 5 —, indicates a marked focusing of attention on x. This implies that the shift of attention becomes more difficult. This phenomenon is caused by the strong inhibition suffered by the SN — see Figure 4b —, coming from the NAcc projection. The subsequent low level of dopamine released by the SN excites the TRN and, consequently, inhibits T_y. Therefore, the use of nicotine is able to promote an hyper-attentional focusing, thus diminishing the mental flexibility.

We observe that, at 250ms, T_y becomes active again. However, its spiking frequency is lower than in the baseline case. It suggests that the attention keeps highly centered on x, even after a period of hyper focusing.

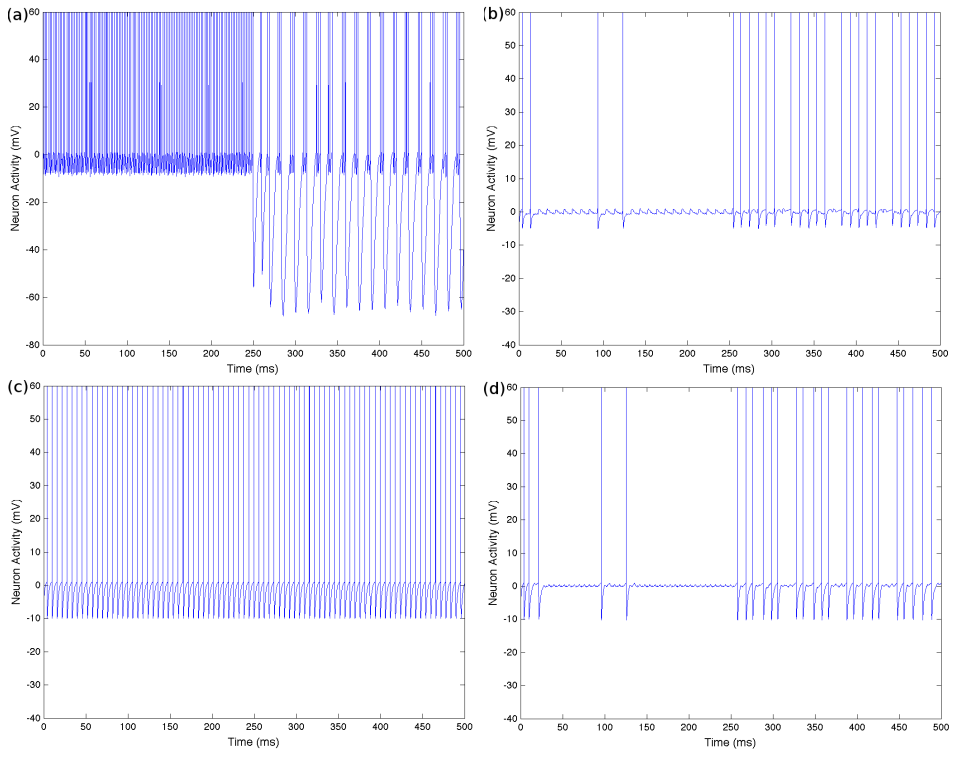

Figure 4: Attention focusing when an individual is exposed to nicotine: (a) VTA dopaminergic neuron spikes in bursts; (b) SN neuron suffers strong inhibition from NAcc; (c) Behavior of T_x; (d) Behavior of T_y.

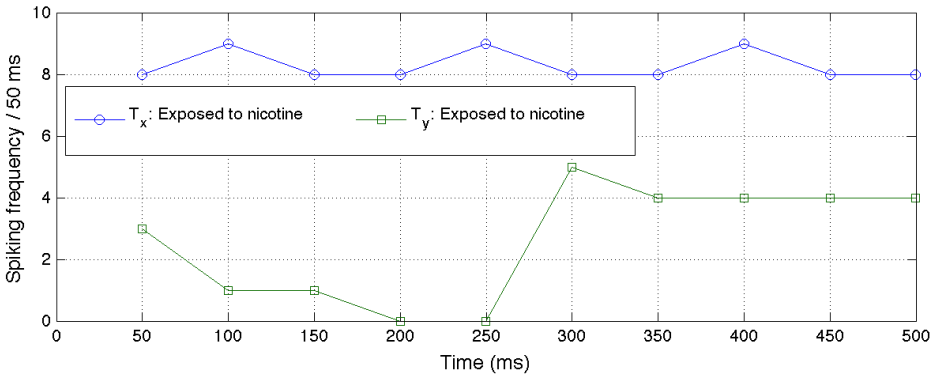

Figure 5: Exposure to nicotine. Spiking frequencies of T_x and T_y.

5.3. Implications in ADHD

Regarding the ADHD, the mesothalamic dopaminergic hypoactivity hinders the attentional shift, enhancing attentional high focusing and mental rigidity [14]. Accordingly, Figure 6a presents the T_y spikes relative to the ADHD *high focusing* condition, with no exposure to nicotine. We may observe that, here, the T_y spiking frequency is much lower than in the baseline condition, shown in Figure 2d. Looking at Figure 6b, we see that up to around 275ms, approximately, the exposure to nicotine aggravates the cognitive impairment.

On the other hand, under the mesothalamic dopaminergic hyperactivity, T_x and T_y show identical neural activity. Consequently, there is a no-winner competition between stimuli x and y, which may lead to distraction or lack of attentional focus. From Figures 7a–b, observe that the T_y spikes under the ADHD *no focusing* condition, without and with nicotine, respectively. This result suggests that the use of nicotine improves the inattention symptom, eliminating the mental lability. It indicates an attentional hyper focusing, followed by a high focusing concentration on stimulus x. Interestingly, the presence of nicotine changes the kind of inattention symptom: from a marked no focusing to a highly centered attentional focus.

6. Discussion

This article presents a neurocomputational model that couples the reward and thalamocortical circuits to investigate how the action of nicotine on the reward circuit influences and modulates the attentional focus. Also,

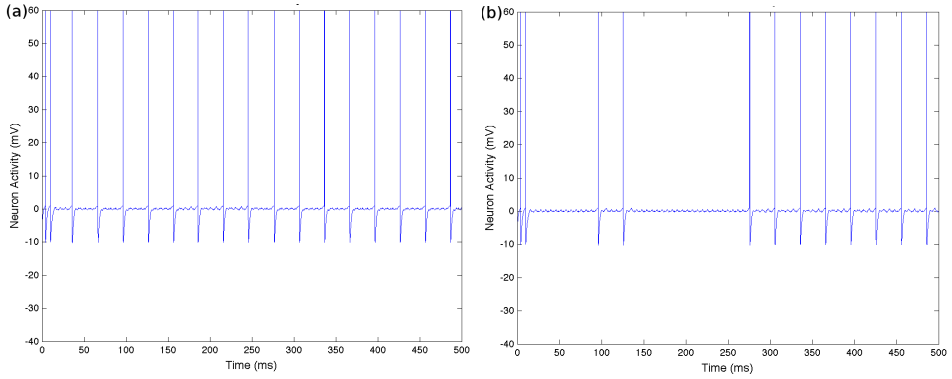

Figure 6: Attention focusing under the ADHD *high focusing* condition: (a) Behavior of T_y with no brain exposure to nicotine; (b) Behavior of T_y under the brain exposure to nicotine.

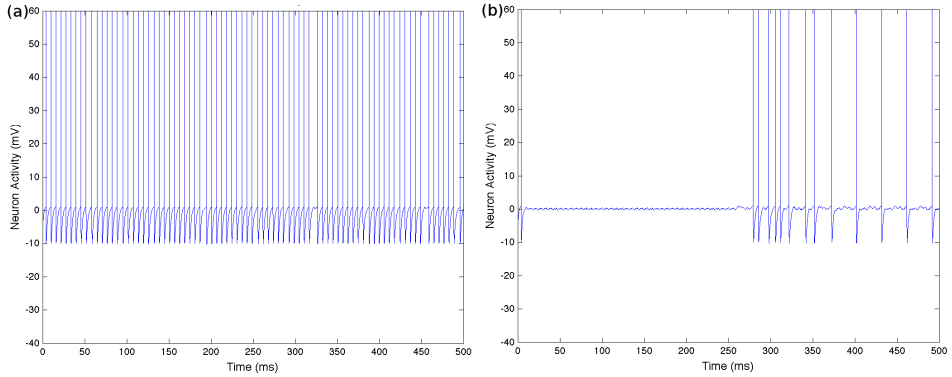

Figure 7: No attention focusing under the ADHD *no focusing* condition: (a) Behavior of T_y with no brain exposure to nicotine; (b) Behavior of T_y under the brain exposure to nicotine.

it addresses possible effects of nicotine in inattention symptoms of ADHD patients.

The high prevalence of smoking among adolescents and adults with ADHD can be interpreted as self-medication for a cognitive dysfunction — inattention — associated with the disorder, since it has been shown that nicotine improves attention in these patients [38]. Several evidences that support this idea include reports from ADHD patients, whereby the acute use of nicotine improves the performance of attention [39], and clinical studies with nicotine patches [6]. Despite experimental evidences, the role of nicotine in improving the focusing of attention is not yet fully elucidated [4, 5, 6].

Our computational simulations suggest that variations in dopamine levels in the reward circuit due to nicotine leads to changes in the nigral dopaminergic activity. As a result, the thalamocortical filtering mechanism is altered, thus hampering the attentional shift.

Starting from a circuit with a dynamics that provides a predefined normal attentional focus, we simulate the influence of nicotine in the reward-thalamocortical system. Our results indicate that nicotine strengthens the focusing of attention on a particular stimulus, and decreases the mental flexibility of smokers. Therefore, they corroborate a number of clinical trials that highlight the role of nicotine in the enhancement of attention [4, 5, 37].

As the thalamocortical circuit involves brain areas related to inattention symptoms observed in ADHD [14], our simulations explicit a mechanism possibly involved in the improvement of attention, triggered by the use of nicotine, in this disorder.

According to simulations presented in [14], decreases in the level of mesothalamic dopamine, in ADHD, lead to an exaggeration in the attention focusing consolidation and a consequent lack of cognitive flexibility. Starting from this point, we simulated the *high focusing* condition and added nicotine to the system. Our results show that, in this particular case, nicotine does not improve such inattention symptom. It even worsens the patient's inability to shift the attentional focus, since promotes attentional hyper focusing.

Finally, we investigated if the presence of nicotine affects the attentional mechanism under the ADHD *no focusing* condition. In this case, the inattention symptom is due to a incapacity of selecting stimuli, caused by a increase in the mesothalamic dopaminergic activity [14]. Our results indicate that ADHD patients which suffer from attentional instability are capable of focusing the attention when exposed to nicotine.

Summarizing, by exploring the interaction between the reward and thalamocortical circuits via SN, we addressed the nicotine's interference on subcortical attentional mechanisms, through its action on the reward system. Our conclusions are in line with the ideas exposed in [8, 10], since the exacerbated attentional focus enhanced by nicotine contributes to the consolidation of habits underlying the act of smoking. Overall, this work highlights how the joint action of cognitive and emotion brain areas permeates the human behavior.

7. Appendix A

Here, in Table 1 we present a list of acronyms used in the text, and in Table 2 we present a glossary of the parameters used in the reward-attention circuit model.

Acronym	**Description**	**Page first described**
ADHD	attention deficit hyperactivity disorder	2
LTP	long term potentiation	4
NAcc	nucleus accumbens	3
nAChR	nicotinic acetylcholine receptors	4
PFC	prefrontal cortex	3
PPN	pedunculopontine nucleus	3
SN	substantia nigra	2
TRN	thalamic reticular nucleus	3
VTA	ventral tegmental area	2

Table 1: Acronyms

Parameter	Description	Value/Unit
C_i	Membrane's capacitance	1 μF.cm^{-2}
E_{K}	Reversal potential of K^+	-80 mV
E_{L}	Reversal potential of I_L	0 mV
β_{K}	Increase rate of g_{K}	150
τ_{K}	Time constant of g_{K}	1,5 ms
g_{L}	Conductance of I_L	10 m.mhos.cm^{-2}
θ	Threshold for sodium channel's opening	1 mV
M	Nicotine decay rate	0,001
k_1	Coefficient of receivers α_7^-	0,5
k_2	Coefficient of receivers α_7^+	4
α_7^-	Amount of receptors not-α_7^+ activated	100
$\mathcal{T}_{max}$	Maximum concentration of neurotransmitters in the synaptic cleft	1 mM
E_{NMDA}	Reversal potential of I_{NMDA}	0 mV
E_{c}	Reversal potential of Ca^{++}	70 mV
$\bar{g}_{\mathrm{c}}$	Increase rate g_{c}	1
$\beta_{[\mathrm{Ca}]}$	Variation rate of calcium concentration	100
$\tau_{[\mathrm{Ca}]}$	Time constant of calcium's pump	500 ms
$\theta_{[\mathrm{Ca}]}$	Threshold to activate I_{ahp}	0.4 mV
β_{ahp}	Increase rate of g_{ahp}	100
τ_{ahp}	Time constant of g_{ahp}	2 ms
g_{pm}	Conductance of pacemaker current	0.29 m.mhos.cm^{-2}
E_{pm}	Reversal potential of	40 mV
$E^{\mathrm{e}}_{\mathrm{sin}}$	Reversal potential of excitatory synapses	40 mV
$E^{\mathrm{i}}_{\mathrm{sin}}$	Reversal potential of inhibitory synapses	-40 mV
$\hat{g}^{\text{c-gvta}}_{\mathrm{sin}}$	Maximal conductance of the synaptic projection cortex-gtva	0.18 m.mhos.cm^{-2}
$\hat{g}^{\text{c-dvta}}_{\mathrm{sin}}$	Maximal conductance of the synaptic projection cortex-dtva	1.3 m.mhos.cm^{-2}
$\hat{g}^{\text{gvta-dvta}}_{\mathrm{sin}}$	Maximal conductance of the synaptic projection gtva-dtva	0.3 m.mhos.cm^{-2}
$\hat{g}^{\text{dvta-nacc}}_{\mathrm{sin}}$	Maximal conductance of the synaptic projection dtva-nacc	0.5 m.mhos.cm^{-}2
$\hat{g}^{\text{nacc-snc}}_{\mathrm{sin}}$	Maximal conductance of the synaptic projection nacc-snc	0,3 m.mhos.cm^{-2}
$\hat{g}^{\text{ppt-snc}}_{\mathrm{sin}}$	Maximal conductance of the synaptic projection ppn-snc	0,2 m.mhos.cm^{-2}
$\hat{g}^{\text{tc-t}}_{\mathrm{sin}}$	Maximal conductance of the synaptic projection cortex-thalamus	0,1 m.mhos.cm^{-2}
$\hat{g}^{\text{t-nrt}}_{\mathrm{sin}}$	Maximal conductance of the synaptic projection thalamus-trn	1,3 m.mhos.cm^{-2}
$\hat{g}^{\text{tc-nrt}}_{\mathrm{sin}}$	Maximal conductance of the synaptic projection cortex-trn	1,3 m.mhos.cm^{-2}
$\hat{g}^{\text{nrt-t}}_{\mathrm{sin}}$	Maximal conductance of the synaptic projection trn-thalamus	0,3 m.mhos.cm^{-2}
$\hat{g}^{\text{ee-t}}_{\mathrm{sin}}$	Maximal conductance of the synaptic projection stimulus-thalamus	0,1 m.mhos.cm^{-2}
t_{pe}	Peak time of excitatory synaptic alpha function	1.5 ms
t_{pi}	Peak time of excitatory synaptic alpha function	1.5 ms
$\hat{g}_{\mathrm{c}}$	Constant regulating increase $g_{\text{k-c}}$	0.4
α	Constant regulating the sigmoid inclination	1
$\hat{g}_{\mathrm{d4}}$	Proportion constant of dopaminergic projection	1 m.mhos.cm^{-2}
t_{pd}	Peak time of D_4 receptor's	2 ms

Table 2: Glossary of parameters

Acknowledgments

The first author acknowledges the Brazilian agency CNPq for the financial support. The second author kindly thanks the CMA-LNCC for the hospitality. The third author thanks the financial support of CNPq, grant numbers 312963/2014-9 and 232677/2014-0 . He also gratefully acknowledges the hospitality of the Division of Applied Mathematics at the Brown University.

References

[1] A. Björklund and S. B. Dunnett, Dopamine neuron systems in the brain: an update, Trends in Neurosciences, vol. 30:(5), 194–202, (2007).

[2] E. S. Bromberg–Martin and M. Matsumoto and O. Hikosaka, Dopamine in motivational control: rewarding, aversive, and alerting, Neuron, vol. 68:(5), 815–834, 2010.

[3] H. D. Mansvelder and D. S. McGehee, Cellular and synaptic mechanisms of nicotine addiction, Journal of Neurobiology, vol. 53, 606–617, (2002).

[4] I. P. Stolerman, N. R. Mirza and M. Shoaib, Nicotine psychopharmacology: Addiction, cognition and neuroadaptation, Medicinal Research Reviews, vol. 15, 47–72, (1995).

[5] E. D. Levin and B. B. Simon, Nicotinic acetylcholine involvement in cognitive function in animals, Psychopharmacology, vol. 138, 217–230, (1998).

[6] A. H. Rezvani and E. D. Levin, Cognitive effects of nicotine. Biological Psychiatry, vol. 49(3), 258–267, (2001).

[7] E. D. Levin and A. H. Rezvani, Nicotine treatment for cognitive dysfunction, Curr Drug Targets CNS Neurol Disord, vol. 1, 423–431 (2002).

[8] J. P. Changeux and B. S. Grurkin and S. Dehaene, A neurocomputacional hypothesis for nicotine addiction, Proceedings of the National Academy of Sciences of the United States of America, vol.103, 1106–1111, (2006).

[9] E. Stefano, Um modelo neurocomputacional da dependência química em nicotina, Dissertação de Mestrado, Coppe/UFRJ, (2005).

[10] S. Metin and N. S. Sengor, From Occasional Choices to Inevitable Musts: A Computational Model of Nicotine Addiction, Computational Intelligence and Neuroscience, doi:10.1155/2012/817485, (2012).

[11] Y.Z. Levy and D.J. Levy and A.G. Barto and J.S. Meyer, A computational hypothesis for allostasis: delineation of substance dependence, conventional therapies, and alternative treatments, Frontiers in Psychiatry, vol.4, Article 167, doi: 10.3389/fpsyt.2013.00167, (2013).

[12] G. M. Shepherd, The synaptic organization of the brain, Oxford University Press, Oxford, (1990).

[13] L. A. V. de Carvalho, Modeling the thalamocortical loop, International Journal of Bio–Medical Computing, vol. 35, 267–296, (1994).

[14] D. Q. M. Madureira, L. A. V. de Carvalho and E. Cheniaux, Attentional focus modulated by mesothalamic dopamine: consequences in parkinson's disease and attention deficit hyperactivity disorder, Cognitive Computation, vol. 2, 31–49, (2010).

[15] R. A. Wise, Brain Reward Circuitry: Insights from Unsensed Incentives, Neuron, vol. 36:(2), 229–240, (2002).

[16] K. Chergui and P. J. Charléty and H. Akaoka and C. F. Saunier and J.-L. Brunet and M. Buda and T. H. Svensson and G. Chouvet, Tonic Activation of NMDA Receptors Causes Spontaneous Burst Discharge of Rat Midbrain Dopamine Neurons In Vivo, European Journal of Neuroscience, vol. 5:(2), 137–144, (1993).

[17] K. Chergui and H. Akaoka and P. J. Charléty and C. F. Saunier and M. Buda and G. Chouvet, Subthalamic nucleus modulates burst firing of nigral dopamine neurones via NMDA receptors, NeuroReport, vol. 5:(10), 137–144, (1994).

[18] F. G. Gonon and M. J. Buda, Regulation of dopamine release by impulse flow and by autoreceptors as studied by in vivo voltammetry in the rat striatum, Neuroscience, vol. 14:(3), 765–774, (1985).

[19] F. G. Gonon, Nonlinear relationship between impulse flow and dopamine released by rat midbrain dopaminergic neurons as studied by in vivo electrochemistry, Neuroscience, vol. 24:(1), 19–28, (1988).

[20] A. J. Bean and R. H. Roth, Extracellular dopamine and neurotensin in rat prefrontal cortex in vivo: effects of median forebrain bundle stimulation frequency, stimulation pattern, and dopamine autoreceptors, The Journal of Neuroscience, vol. 11:(9), 2694–2702, (1991).

[21] H. D. Mansvelder and D. S. McGehee, Long–Term Potentiation of Excitatory Inputs to Brain Reward Areas by Nicotine, Neuron, vol. 27:(2), 349–357, (2000).

[22] J. E. Lisman and J. M. Fellous and X. J. Wang, A role for NMDA-receptor channels in working memory, Nature Neuroscience, vol. 1, 273–275, (1998).

[23] B. W. Connors and M. J. Gutnick and D. A. Prince, Electrophysiological properties of neocortical neurons in vitro, Journal of Neurophysiology, vol. 48:(6), 1302–1320, (1982).

[24] D. A. McCormick and B. W. Connors and J. W. Lighthall and D. A. Prince, Comparative electrophysiology of pyramidal and sparsely spiny stellate neurons of the neocortex, Journal of Neurophysiology, vol. 54:(4), 782–806, (1985).

[25] W. Gerstner and W. M. Kistler, Spiking neuron models: single neurons, populations, plasticity, Cambridge UK: Cambridge University Press, 94–105, (2002).

[26] R. J. MacGregor, Neural and brain modeling, San Diego: Academic Press Incorporation, (1987).

[27] R. J. MacGregor and R. M. Oliver, A model for repetitive firing in neurons, Biol Cybern, vol. 16, 53–64, (1974).

[28] L. A. V. Carvalho and V. L. Roitman, A computational model for the neurobiological substrates of visual attention, International Journal of Bio-Medical Computing, v. 38, 33–45, (1995).

[29] C. E. Jahr and C. F. Stevens, A quantitative description of NMDA receptor-channel kinetic behavior, J. Neuroscience, vol. 10, 1830–1877, (1990).

[30] B. Floran and L. Floran and D. Erlij and J. Aceves, Activation of dopamine D4 receptors modulates [3H]GABA release in slices of the rat thalamic reticular nucleus, Neuropharmacology, vol. 46, 497–503, (2004).

[31] K. D. Guimarães, Influência da nicotina no foco de atenção: um modelo neurocomputacional para os circuitos da recompensa e tálamo-cortical, Tese de Doutorado em Modelagem Computacional, LNCC, (2015).

[32] W. L. Inglis, M. C. Olmstead and T. W. Robbins, Selective deficits in attentional performance on the 5-choice serial reaction time task following pedunculopontine tegmental nucleus lesions, Behavioural Brain Research, vol. 123(2), 117 – 131, (2001).

[33] W. L. Inglis and M. C. Olmstead and T. W. Robbins, pedunculopontine tegmental nucleus lesions impair stimulus-reward learning in autoshaping and conditioned reinforcement paradigms, Behavioral Neuroscience, vol. 114(2), 285–294, (2000).

[34] T. Sleekier and W. I. and P. Winn and A. Sahgal, The pedunculopontine tegmental nucleus: a role in cognitive processes?, Brain Research Reviews, vol. 19:(3), 298 – 318, (1994).

[35] B. Lavoie and A. Parent, Pendunculopontine nucleus in the squirrel monkey: cholinergic and glutamatergic projections to the substantia nigra. J Comp Neurol 1994c; 344: 232–241.

[36] P. A. Pahapill and A. M. Lozano, The pedunculopontine nucleus and Parkinson's disease, Oxford University Press, vol. 123:(9), 1767–1783, (2000).

[37] N. Sherwood, Effects of nicotine on human psychomotor performance, Human Psychopharmacology: Clinical and Experimental, vol. 8:(3), 155–184, (1993).

[38] E. D. Levin, Nicotinic systems and cognitive function, Psychopharmacology, vol. 108:(4), 417–431, (1992).

[39] O. F. Pomerleau and K. K. Downey and F. W. Stelson and C. S. Pomerleau, Cigarette smoking in adult patients diagnosed with attention

deficit hyperactivity disorder, Journal of Substance Abuse, vol. 7:(3), 373–378, (1995).